

Published in final edited form as:

Cell. 2012 September 28; 151(1): 181–193. doi:10.1016/j.cell.2012.09.002.

Asymmetrically Modified Nucleosomes

Philipp Voigt¹, Gary LeRoy², William J. Drury III¹, Barry M. Zee^{2,§}, Jinsook Son¹, David Beck¹, Nicolas L. Young^{2,#}, Benjamin A. Garcia^{2,§}, and Danny Reinberg^{1,*}

¹Howard Hughes Medical Institute, New York University School of Medicine, Department of Biochemistry, 522 First Avenue, New York, NY 10016, USA

²Princeton University, Department of Molecular Biology, 415 Schultz Laboratory, Princeton, NJ 08544, USA

SUMMARY

Mononucleosomes, the basic building blocks of chromatin, contain two copies of each core histone. The associated posttranslational modifications regulate essential chromatin-dependent processes, yet whether each histone copy is identically modified *in vivo* is unclear. We demonstrate that nucleosomes in embryonic stem cells, fibroblasts, and cancer cells exist in both symmetrically and asymmetrically modified populations for histone H3 lysine 27 di/trimethylation (H3K27me_{2/3}) and H4K20me₁. To explore implications of nucleosomal asymmetry, we analyzed co-occurrence of histone marks and obtained direct physical evidence for bivalent nucleosomes carrying H3K4me₃ or H3K36me₃ along with H3K27me₃, albeit on opposite H3 tails. Bivalency at target genes was resolved upon differentiation of ES cells. Polycomb Repressive Complex 2-mediated methylation of H3K27 was inhibited when nucleosomes contain symmetrically, but not asymmetrically, placed H3K4me₃ or H3K36me₃. These findings uncover a potential mechanism for the incorporation of bivalent features into nucleosomes and demonstrate how asymmetry might set the stage to diversify functional nucleosome states.

INTRODUCTION

The nucleosome represents the smallest unit of chromatin structure, consisting of 147 bp of DNA wrapped around a histone octamer that contains two copies each of the core histones H2A, H2B, H3, and H4 (Luger et al., 1997). Histones are subject to a variety of posttranslational modifications (PTMs) (Bannister and Kouzarides, 2011). These modifications have been shown to act as key regulators of gene expression, DNA repair, and many other essential chromatin-associated processes by directly modulating chromatin structure and recruiting effector proteins that harbor PTM-specific binding domains (Bannister and Kouzarides, 2011; Campos and Reinberg, 2009; Taverna et al., 2007).

© 2012 Elsevier Inc. All rights reserved.

*Correspondence should be addressed to D.R.: danny.reinberg@nyumc.org.

§present address B.M.Z., B.A.G.: Epigenetics Program, Department of Biochemistry and Biophysics, Perelman School of Medicine University of Pennsylvania, 1009C Stellar-Chance Laboratories, 422 Curie Boulevard, Philadelphia, PA 19104, USA

#present address N.L.Y.: Ion Cyclotron Resonance Program, National High Magnetic Field Laboratory, Florida State University, 1800 E. Paul Dirac Drive, Tallahassee, FL 32310, USA

SUPPLEMENTAL INFORMATION

The Supplemental Information includes Extended Experimental Procedures, five figures and two tables.

Publisher's Disclaimer: This is a PDF file of an unedited manuscript that has been accepted for publication. As a service to our customers we are providing this early version of the manuscript. The manuscript will undergo copyediting, typesetting, and review of the resulting proof before it is published in its final citable form. Please note that during the production process errors may be discovered which could affect the content, and all legal disclaimers that apply to the journal pertain.

Histone PTMs rarely function in isolation but act in the context of other histone marks, other histones within the nucleosome, and neighboring nucleosomes. A range of effector proteins have been described that contain multiple binding domains for the same or different histone modifications (Ruthenburg et al., 2007). Moreover, effector proteins often form multimeric complexes that bring together different binding modules, as described e.g. for the TFIID complex (Vermeulen et al., 2007). Such multivalency can also be achieved through homomultimerization of histone binding proteins. In these cases, recognition of multiple binding determinants thermodynamically enhances binding affinity and also specificity (Voigt and Reinberg, 2011). In light of these observations, it is critical to establish which combinations of histone marks occur within the same nucleosome *in vivo* and whether a mark is present on both histone copies per nucleosome or only one.

A wealth of information regarding the genomic localization of histone PTMs has been derived from genome-wide chromatin immunoprecipitation (ChIP) studies, which also point to many correlations between modifications (Wang et al., 2008). A special case is the so-called ‘bivalent domain’ that contains histone H3 lysine 4 trimethylation (H3K4me3), a mark associated with active transcription, along with the repressive mark H3K27me3. Such bivalent domains are found at developmentally regulated gene promoters, predominantly in embryonic stem (ES) cells but also in other cell types (Bernstein et al., 2006; Fisher and Fisher, 2011; Mikkelsen et al., 2007). Both the nucleosomal conformation of these bivalent sites as well as the mechanism for their establishment have yet to be resolved. Whereas ChIP studies are highly informative regarding the genomic localization and the correlation of different marks, they usually cannot establish physical co-existence of marks on the same nucleosome nor discriminate between the tails of sister histones within a nucleosome.

Based on multiple lines of evidence, histone marks have been proposed to carry epigenetic information, and several theories have been put forward as to how histone modification patterns might be faithfully transmitted to daughter cells upon cell division (Kaufman and Rando, 2010; Margueron and Reinberg, 2010; Probst et al., 2009). These models postulate that parental histones act as templates for histone modifying enzymes in restoring the original modification patterns to newly replicated chromatin in a faithful manner. Lysine methylation and acetylation on H3 and H4 are the major candidates for epigenetic histone marks. The H3–H4 tetramer can either be segregated as a tetramer, randomly deposited onto the two daughter strands, or as two H3–H4 dimers, generated by the histone chaperone Asf1 (Ransom et al., 2010), which would allow inheritance of marks in a semi-conservative fashion. Although most studies argue against a splitting model, the question remains contested, and mechanisms of inheritance are largely unresolved at present. Several theories for histone mark inheritance, especially the semi-conservative model involving re-deposition of parental H3–H4 dimers, require histones to carry identical modifications on both copies within a nucleosome (Margueron and Reinberg, 2010; Probst et al., 2009).

Given the apparent symmetry of the nucleosome, the two copies of each core histone are commonly considered to be interchangeable and identical. However, the validity of this assumption has thus far evaded experimental scrutiny. The symmetry state of a given histone modification within the nucleosome *in vivo* has remained elusive, rendering it a long-standing question in chromatin biology. We set out to devise an approach for the investigation of modification symmetry and demonstrate that a significant proportion of nucleosomes are asymmetrically modified in ES cells, mouse embryonic fibroblasts (MEFs), and HeLa cells with respect to two prominent histone modifications, H3K27me2/3 and H4K20me1.

RESULTS

An Approach to Analyze Histone Modification Symmetry

To analyze whether sister histones in nucleosomes are symmetrically or asymmetrically modified *in vivo*, we devised a strategy that is based on affinity purification of micrococcal nuclease (MNase)-generated mononucleosomes using modification-specific antibodies. Purification is followed by liquid chromatography (LC)-coupled MS analysis to quantify the abundance of histone modifications. MS-based quantification is performed by chromatographic peak integration, with MS/MS data providing unambiguous assignment of peptide identities and modification states (Plazas-Mayorca et al., 2009). Advances in MS instrumentation have made such approaches feasible, and work by several groups in recent years has shown that histone modifications can be reliably quantified in that way (see e.g. Garcia et al., 2007b; Peters et al., 2003; Syka et al., 2004 for early examples). With respect to a single modification, nucleosomes in chromatin can potentially exist in one of three states – unmodified, modified on one, or both sister histones (Figure 1A). Given specificity of an antibody for that modification, immunoaffinity purification of mononucleosomes exclusively yields nucleosomes that carry the modification on at least one sister histone, while eliminating unmodified nucleosomes. After derivatization and tryptic digest of histones, the relative abundance of the modification is quantified for the antibody-selected nucleosomes by LC-coupled MS/MS analysis. One of three outcomes is expected as follows: In the case of a symmetric modification, all peptides containing the candidate site would be detected as modified (Figure 1A, left panel). In the asymmetric case, unmodified peptides would originate from sister histones that are co-purified with modified histones (Figure 1A, right panel), such that the modified peptide comprises only 50% (Figure 1B). However, if the nucleosome population comprises both symmetrical and asymmetrical versions, the modified peptide would amount to between 50% and 100%, with its abundance directly corresponding to the relative extent of symmetric versions (Figure 1C). The peptides generated and sites covered in our analysis are shown in Figure 1D.

To test our approach, we generated chemically modified histones containing methyl-lysine analogues (MLAs) (Simon et al., 2007) and assembled them into recombinant histone octamers that contained the H3K27me3 mark either on one or both copies of H3 with the help of epitope-tagged versions of H3 (see Extended Experimental Procedures). As expected, in the symmetric case only the trimethylated form of the H3(27-40) peptide could be detected (Figure S1A), whereas the asymmetric case yielded both the trimethylated and the unmodified peptide (Figure S1B) in close to equal abundance. We further subjected mixtures of H3K27me3- and H4K20me1-MLA-containing histone octamers to SDS-PAGE and subsequent sample preparation. We observed very good correlation between expected and observed values over a wide range of ratios (Figure S1C), confirming the well-established reliability of LC-MS/MS-based relative quantification of histone modifications in our experimental setting.

To investigate histone modification symmetry in a range of different cell types *in vivo*, we prepared mononucleosomes from ES, MEFs, and HeLa cells by MNase digestion with two independent preparations per cell type. Subsequent sucrose gradient centrifugation (see Figure S1D for a representative fractionation) yielded essentially pure preparations with on average 93.5% mononucleosomes, containing traces of dinucleosomes (Figure S1E). For reference, the modification patterns of the mononucleosome preparations were determined by LC-MS/MS analysis (Table S1).

Nucleosomes are Modified with H3K27me2/3 both Symmetrically and Asymmetrically

We first applied this methodology to probe for the symmetry of the repressive modification H3K27me3, catalyzed by PRC2. Trimethylation of H3K27 is a pivotal mark in the establishment and maintenance of repressive chromatin states from early development to adulthood (Margueron and Reinberg, 2011; Simon and Kingston, 2009). A prerequisite for the success of our approach is that the modification-directed antibodies must be highly specific. We compared several H3K27me3-specific antibodies by Western blot using MLA histones. Only a single antibody (in-house generated monoclonal 7B11) was rigorously specific for the higher degrees of H3K27 methylation, detecting only H3K27me2/3 while not cross-reacting with H3K9 methylation (Figure S2A). Of note, no material was immunoprecipitated from mononucleosomes prepared from *Eed*^{-/-} ES cells, which are virtually devoid of H3K27me2/3, underscoring antibody specificity (Figure 2A). To analyze modification symmetry, the antibody should further exhibit comparable affinity for mononucleosomes containing one or two H3K27me2/3 marks. Indeed, using recombinant, defined symmetric or asymmetric mononucleosomes in immunoprecipitations (IPs), the antibody was similarly effective (Figure S2B). Moreover, detection of H3K27me2/3 was unaffected by the presence of other modifications such as H3K4me3 or H3K36me3 on the same H3 tail (Figure S2C).

H3K27me2/3-modified mononucleosomes (from here on referred to as H3K27me2/3 nucleosomes) were immunoprecipitated with the 7B11 antibody (Figure 2A) and subjected to LC-MS/MS analysis. Surprisingly, immunoprecipitated H3K27me2/3 nucleosomes exhibited significant amounts of histones carrying either unmodified or monomethylated H3K27 irrespective of cell type (Figure 2B). These findings indicate that a significant amount of mononucleosomes is asymmetrically modified *in vivo*. For H3K27me2/3 nucleosomes in E14 ES cells, ~79±2% of all H3 tails contain the H3K27me2/3 mark, whereas ~21±2% are either unmethylated or monomethylated, yielding ~58±3% of symmetric and ~42±3% asymmetric nucleosomes. Similar levels of asymmetry were observed for HeLa cells, MEFs, and an additional ES cell line (Figure 2B). Taken together, nucleosomes exhibit both symmetric and asymmetric H3K27 modification *in vivo*.

H4K20me1 also Exists Asymmetrically

To probe symmetry for another histone PTM, we analyzed H4K20me1, which is established by PR-Set7 and participates in chromosome condensation during mitosis, the DNA damage response, and has been correlated with both actively transcribed and repressed genes (Beck et al., 2012). A commercially available antibody proved to be specific for H4K20me1 as no cross-reactivity was observed with other methylation sites, and acetylation at H4K16 did not interfere with IP (Figure S2D, F). Importantly, histones isolated from 4-hydroxytamoxifen treated MEFs with a *PR-Set7*^{flox}; *CRE*^{ERT} genotype (Oda et al., 2009) did not exhibit reactivity with this antibody in Western blots (Figure S2E).

Similar to our observations for H3K27 methylation, H4K20me1 nucleosomes contain significant amounts of unmodified or dimethylated H4K20. For H4K20me1 nucleosomes from ES cells, H4K20me1 amounts to 75±2%, indicating a roughly equal proportion of symmetric and asymmetric nucleosomes in this cell type (Figure 2C). Both MEFs and HeLa cells contain slightly, but not significantly higher percentages of symmetric H4K20me1 nucleosomes (Figure 2C). We thus confirmed the existence of asymmetric modification for an additional histone mark on a different histone. Investigation of additional marks was not tenable at this time, as the corresponding antibodies tested were insufficiently specific in Western blots or failed to significantly enrich their target sites in IP (data not shown).

A Model for Nucleosomal Asymmetry

Our results indicate that asymmetry of histone modifications might be a general, hitherto unrecognized feature of nucleosomes *in vivo*. Given the abundance of asymmetric nucleosomes, we asked whether a random distribution of modified histones into nucleosomes could explain asymmetry. To this end, we calculated the proportion of unmodified, asymmetrically, and symmetrically modified nucleosomes from a simple binomial distribution. In this model, the distribution of nucleosome populations is governed by the overall amount of modified histones (parameter p , Figure S3A). For E14 ES cells, the overall abundance of H3K27me_{2/3} was 42±2% (Figure 2B). A random distribution would result in 48.7% and 17.6% of asymmetrically and symmetrically modified nucleosomes, respectively (Figure S3C). Correspondingly, symmetric nucleosomes would account for only 26% of all modified nucleosomes. The disagreement with experimentally observed levels of symmetry in this and other cases (Figure S3C) argues against a random distribution of modified histones.

We thus considered an alternative model to explain modification asymmetry. In this 'reaction model' (Figure S3B), the placement of PTMs is treated as a two-step reaction process. An initial recruitment step controls whether a nucleosome will be modified on one histone copy. This step and its efficiency are either governed by cellular factors or of a stochastic nature. In the next step, a second modification per nucleosome is placed with a probability q that determines the degree of symmetry. Assuming 50% efficiency in each step, this model predicts 50% unmodified nucleosomes and 25% each asymmetrically and symmetrically modified nucleosomes (i.e. 50% symmetry), leading to 37.5% modified tails overall. These values are in reasonable agreement with the experimental data. With fitting of both parameters, the model can predict the experimental data with high accuracy (Figure S3C). We conclude that nucleosomal asymmetry may be direct consequence of inherent properties of the histone modifying complexes, even though more complex factors may be involved as well.

Co-Occurrence of H3K27me₃ and H3K4me₃ within a Nucleosome

Among several potential implications for nucleosomal structure and function, asymmetrical modification may increase the range of attainable histone mark combinations. Of special importance are the so-called bivalent domains featuring positive H3K4me₃ marks and repressive H3K27me₃ marks (Fisher and Fisher, 2011; Mikkelsen et al., 2007). Yet these marks have been shown to hardly ever coexist on individual histone tails (Young et al., 2009), and the presence of H3K4me₃ and H3K36me₃ was reported to inhibit PRC2 (Schmitges et al., 2011). Since the architecture of nucleosomes at bivalent loci remains elusive, we attempted to probe the physical co-occurrence of the relevant marks. Moreover, the LC-MS/MS analysis of H3K27me_{2/3} and H3K4me₃ nucleosomes provides direct information on the overall average modification pattern of nucleosomes from repressive and active environments, respectively.

For H3K27me_{2/3} nucleosomes purified from E14 ES cells, we observed a concomitant occurrence of other repressive marks such as H3K9me_{2/3} and H4K20me₂, whereas acetylation was reduced at multiple sites on H3 and H4 (Figure 3A and Table S2). Complementing these observations, ChIP-seq studies have shown that di/trimethylation of H3K9 and H3K27 tend to colocalize and that these regions are also largely devoid of acetylation (Wang et al., 2008). H3K36me_{2/3}, found in actively transcribed genes, was—although markedly decreased—nonetheless present in H3K27me_{2/3} nucleosomes (Figure 3A). Similar observations were made for MEFs and HeLa cells (Figure 3C and Table S2). Nucleosomes featuring both H3K27me_{2/3} and higher H3K36 methylation might arise from domains containing bivalent or poised genes expressed at low levels or from domains of a

recently described class of expressed genes with mainly promoter-associated H3K27me3 (Young et al., 2011).

The H3K4me2/3-containing peptides could not be accurately quantified in our approach due to their low hydrophobicity and limited interaction with the C18 resin used. However, we addressed this limitation by probing for H3K27me2/3 on nucleosomes affinity-purified with an H3K4me3 antibody (Figure S2G). This antibody significantly enriched its target mark in IP, albeit not to a population homogeneously modified with H3K4me3. H3K4me3 mononucleosomes from all cell types analyzed exhibited strong co-enrichment with acetylation marks on both H3 and H4 (Figure 3B and Table S2). Moreover, H3K79me2 was markedly enriched on all H3K4me3 nucleosomes (Figure 3B). In agreement, genome-wide studies observed co-localization of H3K4me3 with acetyl marks and H3K79me2 methylation at regions surrounding transcriptional start sites (Wang et al., 2008). Conversely, methylation at H3K9 was pronouncedly reduced. Interestingly, H3K27me2/3 methylation levels remained largely unchanged in ES cells (Figure 3B), whereas a reduction in H3K27me2/3 was observed for H3K4me3 nucleosomes in MEFs (Figure 3D). These observations demonstrate the existence of H3K27me3 and H3K4me3 within the same nucleosomes in ES cells, and to a lesser extent in more differentiated cell types such as MEFs. Our data thus provides direct evidence for the existence of bivalent nucleosomes.

We performed a similar modification analysis for H4K20me1 nucleosomes from ES cells, observing reductions in H3K9me2/3 and slight increases in activating marks such as H3K4me1 and H3K36me2/3 (Figure S4 and Table S2). Of note, the neighboring and potentially antagonizing H4K16ac mark was present alongside H4K20me1 and even slightly enriched. Taken together, the modification pattern of H4K20me1 nucleosomes is compatible with existence of this mark with H4K16ac in open chromatin and on active genes, which has been suggested by ChIP-Seq studies (Wang et al., 2008).

H3K4me3 and H3K27me3 Map to Single Nucleosomes at Bivalent Promoters and Resolve Upon Differentiation

As our MS-based data demonstrates that mononucleosomes containing both H3K4me3 and H3K27me3 exist *in vivo*, we aimed to complement these findings with sequential ChIP (re-ChIP) experiments. In contrast to LC-MS/MS, re-ChIP experiments lack quantitative information on modifications, but provide information on their localization within the genome. To ensure stable interactions during purification and re-CHIP steps, mononucleosomes were crosslinked immediately after MNase digestion. Our monoclonal H3K27me2/3 antibody exhibited diminished reactivity on crosslinked material (data not shown). We thus employed a widely used H3K27me3 ChIP antibody exhibiting minor cross-reactivity with H3K9me3 (Figure S2H) along with an antibody against H3K4me3 (see Figure S2I for specificity). In line with the detection of both marks in conventional ChIP experiments, we observed enrichment at the promoters of the *Gata4*, *Hoxb13*, *Hoxc5*, and *Olig1* genes in re-ChIP for H3K27me3 followed by H3K4me3 (Figure 4A). As a control, the exclusively H3K4me3-marked promoters of *Pou5f1*, *Polm*, and *Gapdh* did not exhibit enrichment over control IPs in re-ChIP (Figure 4A). Upon differentiation with retinoic acid, H3K27me3 is reduced at the *Gata4*, *Hoxb13*, and *Hoxc5* promoters, which concomitantly show diminished enrichment in re-ChIP (Figure 4B). In contrast, the *Olig1* promoter retains both H3K27me3 and H3K4me3 under these conditions and remains positive in re-ChIP (Figure 4B). Taken together, nucleosomes carrying both H3K4me3 and H3K27me3 occur at relevant genomic loci, where they likely function to keep genes in a poised state in undifferentiated cells. These findings support the prevalent view on bivalent domains.

To probe for global changes in asymmetry and co-occurrence of marks on H3K27me2/3 nucleosomes in the differentiation process, we affinity-purified H3K27me2/3 nucleosomes

from retinoic acid-treated cells and analyzed their modification status by LC-MS/MS. H3K27me_{2/3} nucleosomes from treated cells exhibited a marginal, non-significant decrease in overall symmetry (Figure 4C). We observed that those nucleosomes were further depleted for acetylation at H4 and some sites on H3, while the repressive H3K9me_{2/3} and H4K20me₃ marks were elevated compared to the already high levels found on H3K27me_{2/3} nucleosomes in untreated cells (Figure 4D). These findings indicate that active and repressive regions might further resolve upon differentiation.

PRC2 is Inhibited by Symmetric but Not Asymmetric Active Methyl Marks

As described above, we observed the co-occurrence of H3K27me_{2/3} with H3K4me₃ and H3K36me₃ within nucleosomes (Figure 3, Table S2), even though occurrence of these marks within the same histone tail has been shown to be strongly disfavored (Young et al., 2009; Yuan et al., 2011). To further investigate the interplay between these marks, we analyzed the activity of PRC2 on oligonucleosomal substrates carrying trimethylation marks at defined sites on one or both copies of H3. The presence of asymmetric H3K27me₃ stimulated PRC2 activity towards the unmodified H3 copy (Figure 5A), in line with our observations that H3K27me₃ stimulates PRC2 activity (Margueron et al., 2009). In agreement with recent studies (Schmitges et al., 2011; Yuan et al., 2011), PRC2 failed to efficiently methylate nucleosomes that carry H3K4me₃ or H3K36me₃ in a symmetric fashion (Figure 5A, B, upper panel). In contrast, PR-Set7-mediated methylation of these nucleosomes at H4K20 was not adversely affected (Figure S5A). Intriguingly, PRC2-mediated methylation was unaffected if H3K4me₃ or H3K36me₃ were present only on one H3 copy (Figure 5A, B, lower panel). In conclusion, these findings provide a rationale for the establishment of nucleosomes carrying both activating marks and repressive H3K27me₃ as found in bivalent domains and detected in our analysis.

PRC2 activity on symmetrically modified H3K4me₃/H3K36me₃ nucleosomes might be precluded either by diminished binding of PRC2 or by direct effects on catalysis. We thus analyzed binding of PRC2 to symmetrically and asymmetrically modified mononucleosomes. PRC2 was found to interact with both types of nucleosomes without any overt differences (Figure S5B). It has been shown that the Nurf55 (RbAp46/48 in mammals) subunit binds the N terminus of H3, and this binding is abrogated by trimethylation of H3K4 (Schmitges et al., 2011). While not affecting overall nucleosome binding, lack of H3 binding to Nurf55 was proposed to be an allosteric signal eliciting inhibition of the Ezh2 SET domain (Schmitges et al., 2011). Our data on asymmetric nucleosomes suggests that this inhibition requires both tails of H3 to be modified. In addition, binding of the H3 N terminus might be required for proper substrate presentation and thus efficient catalysis.

Mononucleosomes *In Vivo* Carry H3K27me₃ and H3K4me₃/H3K36me₃ on Separate H3 Tails

To test whether the conformation of nucleosomes *in vivo* corresponds to the behavior of PRC2 *in vitro*, we first analyzed the methylation status of H3K36 in H3K27me_{2/3} nucleosomes isolated from ES cells. After tryptic digest, both H3K36 and H3K27 remain connected within a single tryptic fragment, H3(27-40), allowing to directly correlate their modification status on a single histone (Figure 6A). We quantified the relative abundance of H3K36 methylation as a function of the methylation status at H3K27, distinguishing between H3K27me_{0/1} and H3K27me_{2/3}. Strikingly, the bulk of H3K36me_{2/3} was found on peptides devoid of H3K27me_{2/3}, indicating their presence on opposing tails in asymmetric H3K27me_{2/3} nucleosomes *in vivo* (Figure 6B). Upon normalization, it becomes evident that almost all peptides containing H3K27me_{2/3} are either unmodified or monomethylated at H3K36, whereas those without higher methylation at H3K27 contain all states of H3K36 methylation, with H3K36me₂ and H3K36me₃ constituting up to 42% and 5% in ES cells,

respectively (Figure 6C). The exclusion of H3K36me3 from H3K27me2/3 peptides was consistent between all cell types analyzed, whereas H3K27me2/3 nucleosomes exhibited slightly less strict exclusion of H3K36me2 in MEF and HeLa cells (Figure 6C). This observation might be caused by different sets of H3K36me2-catalyzing enzymes in those cells, or auxiliary PRC2 subunits that might modulate sensitivity to H3K36me2.

Conducting a similar analysis of H3K4me3 and H3K27me3 occurrence on separate copies of H3 requires the digestion with Glu-C protease to circumvent the loss of topological information upon trypsin digest. A drawback of the associated Middle-Down MS analysis is a markedly decreased sensitivity as compared to Bottom Up analysis of tryptic fragments, requiring comparatively large amounts of sample. Despite significant scale-up of immunopurifications, we were unable to obtain sufficient material to perform Middle-Down analysis of H3K27me2/3 nucleosomes (data not shown). We therefore turned to acid-extracted histones to investigate the overall co-occurrence of H3K4me3 and H3K27me3. As H3K27me2/3 nucleosomes are a subset of all nucleosomes in the cell, the observations obtained on overall nucleosomes consequently extend to this subclass as well. We digested the histones with Glu-C and analyzed the 1–50 peptide from H3.1 by middle-down LC-MS/MS (Figure 6D). We detected and quantified peptides that are modified at H3K4 and/or H3K27 with a custom-made software followed by manual validation. Small but reliably quantifiable amounts of peptides containing H3K4me3 along with unmodified, acetylated or monomethylated H3K27 were detected (Figure 6E). However, we did not observe any peptides that contain both H3K4me3 and H3K27me3 (Figure 6E). When performing a similar analysis for H3K4me2-containing peptides, we observe marginal quantities of H3K27me3 that make up about 0.3% of all H3K4me2-containing peptides. Even if one assumes that H3K4me2 may theoretically substitute for H3K4me3, the observed peptide abundances are vastly too low to account for the ~15% bivalent promoters in ES cells (Mikkelsen et al., 2007). Taken together, these findings suggest that, in bivalent nucleosomes, H3K4me3 and H3K27me3 reside on distinct copies of H3 in an asymmetric fashion *in vivo*.

DISCUSSION

The relationship between sister histones and the accessible space of PTM combinations in a nucleosome are key to the establishment of PTM patterns, the means by which they convey information, and their potential inheritance. In this study, we devised a method to address histone mark symmetry and provide evidence that sister histones are not necessarily identical within a nucleosome. This asymmetry in histone modifications might be a general, hitherto unrecognized, feature of nucleosomes *in vivo*.

Experimental Challenges of Probing Nucleosomal Asymmetry

Addressing the status of histone PTMs on sister histones has so far been hampered by the absence of adequate techniques. A recent report showed that H3 can be methylated at H3K27 even if the sister histone within a nucleosome carries a K27A mutation, which was interpreted as an indication of nucleosome asymmetry (Chen et al., 2011). We suggest that this observation reflects the capability of the enzyme to methylate such a substrate, but may not allow conclusions regarding the *in vivo* symmetry state. The data presented here were obtained on native nucleosomes and directly assess symmetry. In the case of ChIP analyses, co-correlation of different marks at genomic loci can be assessed in cell populations, but their physical co-existence on the same nucleosome cannot be established. An exception is sequential ChIP performed on native, purified mononucleosomes. Although these assays have been performed e.g. in the context of bivalent domains (see below), reports describing their application to the different modification states of a single site are scarce. Based on such experiments, H3K4me3 and H3K4me2 have been suggested to co-occur within nucleosomes

(Kouskouti and Talianidis, 2005). However, results of this and other re-ChIP studies need to be interpreted cautiously, as insufficient antibody specificity, incomplete removal of the initial antibody, and contamination with oligomeric nucleosomes can compromise results. The affinity purification-based LC-MS/MS analysis described in this study allowed us to overcome these limitations and enabled us to assess the symmetry state of nucleosomes *in vivo* in a quantitative manner.

Asymmetry of H3K27me2/3 and H4K20me1

We observed asymmetry for two major histone modifications in several cell lines. Even though antibody specificity issues precluded analysis of further histone PTMs, we speculate that asymmetry may not be restricted to H3K27me3 and H4K20me1. Indeed, our data implies that H3K4me3 and H3K36me3 are present in asymmetric fashion as well, at least in the case of bivalent nucleosomes. For both H3K27me2/3 and H4K20me1, differences were small and mostly non-significant between cell types and the two marks, indicating that overall asymmetry may be controlled by characteristics inherent to the modifying enzymes PRC2 and PR-Set7. Our reaction model explains the observed proportions of asymmetric nucleosomes quantitatively (Figure S3B). A recruitment step coupled with a first methylation may be followed by a second reaction with a certain propensity. The nature of the recruitment is irrelevant in this model, and may in theory be purely stochastic or governed by specific recruitment mechanisms. It is unclear at present how the degree of symmetry is controlled and whether factors exist that modulate symmetric placement of histone PTMs. The exclusively asymmetric conformation of H3K27me3 at bivalent promoters may represent a special case where the presence of another mark imposes asymmetry. Identifying factors that globally or locally control the degree of symmetry may enable us to modulate asymmetry *in vivo*, greatly facilitating further exploration of its implications.

Nucleosomal Asymmetry May be Key to the Establishment of Bivalent Domains

Bivalent domains constitute a unique chromatin signature found at many gene promoters primarily in ES cells. Their existence has been demonstrated both by conventional genome-wide ChIP analysis and re-ChIP studies. Those were mostly performed on crosslinked, sonicated chromatin fragments (Bernstein et al., 2006), but also on native MNase-digested chromatin consisting primarily—but not exclusively—of mononucleosomes (Seenundun et al., 2010). The use of material containing oligonucleosomes left the formal possibility that those marks reside on neighboring nucleosomes. To unambiguously address the existence on single nucleosomes, the re-ChIP experiments in our study were carried out on purified mononucleosomes. In agreement with the interpretation of earlier studies, our data corroborates that H3K4me3 and H3K27me3 coexist on the same nucleosomes at gene promoters. However, re-ChIP cannot distinguish between the different tails of sister histones. Our novel strategy allowed us not only to provide quantitative information of many histone PTMs in parallel, but also to distinguish between the sister histones in a nucleosome for the marks involved in bivalent domains by employing both bottom-up and middle-down MS approaches. Our findings provide insight into the architecture of bivalent nucleosomes and indicate an elegant solution through placement of the marks on separate tails of H3, allowing co-occurrence on single nucleosomes.

To explore the mechanistic basis for the generation of such bivalent nucleosomes observed *in vivo*, we performed methyltransferase assays with PRC2 *in vitro* on defined, recombinant nucleosomal substrates with active marks being present either symmetrically or asymmetrically. Based on our data, we propose the following working model (Figure 7). PRC2 generates predominantly symmetric nucleosomes if activating marks are absent. If PRC2 encounters asymmetric – but not symmetric – trimethylation at H3K4 or H3K36, it

may place a repressive mark on the opposite tail. This regulation of PRC2 activity provides a rationale for the establishment of bivalent domains. In the transition from ES cells to more differentiated cell types, a proportion of these nucleosomes will be retained at loci that remain poised. Alternatively, they might resolve into nucleosomes carrying either mark in possibly asymmetric or symmetric fashion. Nucleosomes carrying only H3K27me3 remain modified upon differentiation in either symmetric or asymmetric fashion. Our data indicates that the overall extent of asymmetry does not change significantly in e.g. retinoic acid-induced differentiation. This observation was obtained on bulk nucleosomes and reflects overall levels of asymmetry rather than gene promoter-specific asymmetry. Changes in symmetry may nonetheless occur at specific loci, such as resolved bivalent promoters where symmetry might be restored, or at loci that become inaccessible to PRC2, increasing asymmetry. Besides the active marks H3K4me3 and H3K36me3, other factors likely control asymmetry on bulk nucleosome populations. Among them, bound effector proteins at other sites, for instance HP1 at H3K9, may diminish accessibility to the second H3 copy, leading to indirect effects on PRC2 activity.

Potential Implications of Nucleosomal Asymmetry Beyond Bivalent Domains

Exactly how the singular, asymmetric presentation of a histone mark within a nucleosome affects its function and recognition in the context of other histone marks is currently unknown. For example, the presence of a single H3K27me2/3 mark per nucleosome might be sufficient to retain a repressed chromatin state. Conversely, a single H3K4me3 mark might still allow recruitment of effector proteins such as TFIID, albeit with potentially lower affinity or altered kinetics. The modification status on the other tail may be of importance as well, as e.g. unmodified H4K20 and the repressive H4K20me2 mark may differ in their influence on H4K20me1. Cell types with overall higher H4K20me2 levels also exhibited stronger pairing of H4K20me1 with H4K20me2 (Figure 2, Tables S1, S2), indicating activity of the Suv4-20 enzymes as a regulatory element in that case. Dimeric proteins such as HP1 might experience a greater impact on their recruitment and mode of action—especially in the context of chromatin compaction—due to the presence of a single versus two binding sites per nucleosome. The asymmetric features of nucleosomes might also influence the emerging concept of combinatorial recognition of different histone marks (Ruthenburg et al., 2011; Taverna et al., 2007; Vermeulen et al., 2007). In contrast, the stability of a mark at a certain locus is presumably higher if it is present on both sister histones, rendering it more refractive to removal by demethylases, for example.

In considering the stability of a given chromatin domain, the asymmetry between sister histones might significantly impact their potential inheritance. The semi-conservative model postulating segregation of H3–H4 units as dimers relies on the presence of identical sister histones at the onset of replication. At loci featuring asymmetric nucleosomes, this condition is not fulfilled, rendering the general validity of such a mechanism less tenable. In this regard, a recent report shows that splitting of H3–H4 tetramers plays only a minor role in HeLa cells during replication (Xu et al., 2010), and also a range of earlier publications argue against a general splitting of dimers (Annunziato, 2005). Yet, these studies have been performed mainly with transformed cells.

Taken together, we provide direct evidence for the existence of nucleosomes with asymmetric modification states along with symmetrically modified ones in living cells. As a direct consequence of the existence of asymmetric nucleosomes, a semi-conservative model of histone mark inheritance might not generally be applicable. Asymmetric modification, however, provides efficient means to extend the combinatorial space of histone marks. We provide evidence that such a mechanism likely operates in the establishment of bivalency, but other scenarios are conceivable as well. The admixture of symmetrically and

asymmetrically modified nucleosomes might reflect a widespread regulatory device that impacts chromatin biology in ways we have yet to uncover.

EXPERIMENTAL PROCEDURES

Preparation of mononucleosomes and immunoaffinity purification

Mononucleosomes were generated by MNase digestion and sucrose gradient purification based on established protocols (see Extended Experimental Procedures). Sucrose gradient fractions containing more than 90% mononucleosomes were pooled and used for subsequent steps. Mononucleosomes were immunoprecipitated with modification-specific antibodies (5–10 μ g per IP) in IP buffer (50 mM HEPES pH 7.9, 50 mM NaCl, 50 mM KCl, 5 mM EDTA, 0.5% NP-40, 0.1% N-lauroyl sarcosine, 5 mM sodium butyrate). After washing three times with IP buffer, histones were eluted by boiling in SDS sample buffer and separated by SDS-PAGE.

Sample Preparation and Quantitative LC-MS/MS Analysis

Procedures for chemical propionylation and tryptic digest were adapted from previously described solution protocols to in-gel conditions (Garcia et al., 2007a; Plazas-Mayorca et al., 2009). LC/MS analysis and quantification of histone modifications was performed essentially as described (DiMaggio et al., 2009; Plazas-Mayorca et al., 2009). For detailed Bottom Up and Middle Down LC-MS/MS procedures see Extended Experimental Procedures.

ChIP and re-ChIP assays

ChIP assays on purified, crosslinked mononucleosomes were performed as described in the Extended Experimental Procedures. Antibodies used for ChIP were: H3K4me3 (Abcam, ab8580), H3K27me3 (Millipore, 07-449). Primers used for quantitative real-time PCR are given in the Extended Experimental Procedures.

Generation of modified histones and nucleosomes

Recombinant mononucleosomes and chromatin were reconstituted by salt dialysis as described (Margueron et al., 2009). MLAs were introduced into recombinant histones as established previously (Margueron et al., 2009; Simon et al., 2007). Asymmetric octamers containing both unmodified and modified copies of H3 were obtained by reconstitution from H3 carrying N-terminal His and Strep tags, respectively, and subsequent two-step affinity purification (see details in Extended Experimental Procedures).

Histone methyltransferase assays and PRC2 interaction assays

Histone methyltransferase assays and PRC2–nucleosome interaction assays were performed essentially as described (Margueron et al., 2009). If not indicated otherwise, 200 ng of purified PRC2 complex or 50 ng of PR-Set7 were incubated with 1 μ g of reconstituted plasmid-based chromatin for 1 h at 30 °C. For assays using PR-Set7, 50 ng of enzyme purified from *E. coli* was used per reaction. See also Extended Experimental Procedures.

Supplementary Material

Refer to Web version on PubMed Central for supplementary material.

Acknowledgments

We thank Till Bartke and Tony Kouzarides for the H4 Δ (1-27)I28C construct. P.V. is supported by fellowships from the Deutsche Akademie der Naturforscher Leopoldina (LPDS 2009-5) and the Empire State Training Program

in Stem Cell Research (NYSTEM, contract # C026880). Work in the Reinberg laboratory is funded by the Howard Hughes Medical Institute and the National Institute of Health (grants GM064844 and R37GM037120). The Garcia laboratory is supported by grants from the NSF (Early Faculty Career award and CBET-0941143), the American Society for Mass Spectrometry and the NIH Office of the Director (DP2OD007447). We thank Drs. W.-W. Tee and R. Bonasio for helpful discussions and Dr. L. Vales for critical reading of the manuscript.

References

- Annunziato AT. Split decision: what happens to nucleosomes during DNA replication? *J Biol Chem.* 2005; 280:12065–12068. [PubMed: 15664979]
- Bannister AJ, Kouzarides T. Regulation of chromatin by histone modifications. *Cell Res.* 2011; 21:381–395. [PubMed: 21321607]
- Beck DB, Oda H, Shen SS, Reinberg D. PR-Set7 and H4K20me1: at the crossroads of genome integrity, cell cycle, chromosome condensation, and transcription. *Genes & Development.* 2012; 26:325–337. [PubMed: 22345514]
- Bernstein BE, Mikkelsen TS, Xie X, Kamal M, Huebert DJ, Cuff J, Fry B, Meissner A, Wernig M, Plath K, et al. A bivalent chromatin structure marks key developmental genes in embryonic stem cells. *Cell.* 2006; 125:315–326. [PubMed: 16630819]
- Campos EI, Reinberg D. Histones: annotating chromatin. *Annu Rev Genet.* 2009; 43:559–599. [PubMed: 19886812]
- Chen X, Xiong J, Xu M, Chen S, Zhu B. Symmetrical modification within a nucleosome is not required globally for histone lysine methylation. *EMBO Rep.* 2011; 12:244–251. [PubMed: 21331095]
- DiMaggio PA, Young NL, Baliban RC, Garcia BA, Floudas CA. A mixed integer linear optimization framework for the identification and quantification of targeted post-translational modifications of highly modified proteins using multiplexed electron transfer dissociation tandem mass spectrometry. *Mol Cell Proteomics.* 2009; 8:2527–2543. [PubMed: 19666874]
- Fisher CL, Fisher AG. Chromatin states in pluripotent, differentiated, and reprogrammed cells. *Curr Opin Genet Dev.* 2011; 21:140–146. [PubMed: 21316216]
- Garcia BA, Mollah S, Ueberheide BM, Busby SA, Muratore TL, Shabanowitz J, Hunt DF. Chemical derivatization of histones for facilitated analysis by mass spectrometry. *Nat Protoc.* 2007a; 2:933–938. [PubMed: 17446892]
- Garcia BA, Pesavento JJ, Mizzen CA, Kelleher NL. Pervasive combinatorial modification of histone H3 in human cells. *Nat Meth.* 2007b; 4:487–489.
- Kaufman PD, Rando OJ. Chromatin as a potential carrier of heritable information. *Curr Opin Cell Biol.* 2010; 22:284–290. [PubMed: 20299197]
- Kouskouti A, Talianidis I. Histone modifications defining active genes persist after transcriptional and mitotic inactivation. *EMBO J.* 2005; 24:347–357. [PubMed: 15616580]
- Luger K, Mäder AW, Richmond RK, Sargent DF, Richmond TJ. Crystal structure of the nucleosome core particle at 2.8 Å resolution. *Nature.* 1997; 389:251–260. [PubMed: 9305837]
- Margueron R, Justin N, Ohno K, Sharpe ML, Son J, Drury WJ, Voigt P, Martin SR, Taylor WR, De Marco V, et al. Role of the polycomb protein EED in the propagation of repressive histone marks. *Nature.* 2009; 461:762–767. [PubMed: 19767730]
- Margueron R, Reinberg D. Chromatin structure and the inheritance of epigenetic information. *Nat Rev Genet.* 2010; 11:285–296. [PubMed: 20300089]
- Margueron R, Reinberg D. The Polycomb complex PRC2 and its mark in life. *Nature.* 2011; 469:343–349. [PubMed: 21248841]
- Mikkelsen TS, Ku M, Jaffe DB, Issac B, Lieberman E, Giannoukos G, Alvarez P, Brockman W, Kim TK, Koche RP, et al. Genome-wide maps of chromatin state in pluripotent and lineage-committed cells. *Nature.* 2007; 448:553–560. [PubMed: 17603471]
- Oda H, Okamoto I, Murphy N, Chu J, Price SM, Shen MM, Torres-Padilla ME, Heard E, Reinberg D. Monomethylation of histone H4-lysine 20 is involved in chromosome structure and stability and is essential for mouse development. *Mol Cell Biol.* 2009; 29:2278–2295. [PubMed: 19223465]
- Peters AHFM, Kubicek S, Mechtler K, O’Sullivan RJ, Derijck AAHA, Perez-Burgos L, Kohlmaier A, Opravil S, Tachibana M, Shinkai Y, et al. Partitioning and plasticity of repressive histone

- methylation states in mammalian chromatin. *Molecular Cell*. 2003; 12:1577–1589. [PubMed: 14690609]
- Plazas-Mayorca MD, Zee BM, Young NL, Fingerman IM, Leroy G, Briggs SD, Garcia BA. One-pot shotgun quantitative mass spectrometry characterization of histones. *J Proteome Res*. 2009; 8:5367–5374. [PubMed: 19764812]
- Probst AV, Dunleavy E, Almouzni G. Epigenetic inheritance during the cell cycle. *Nat Rev Mol Cell Biol*. 2009; 10:192–206. [PubMed: 19234478]
- Ransom M, Dennehey BK, Tyler JK. Chaperoning histones during DNA replication and repair. *Cell*. 2010; 140:183–195. [PubMed: 20141833]
- Ruthenburg, Alexander J.; Li, H.; Milne, Thomas A.; Dewell, S.; Mcginty, Robert K.; Yuen, M.; Ueberheide, B.; Dou, Y.; Muir, Tom W.; Patel, Dinshaw J., et al. Recognition of a Mononucleosomal Histone Modification Pattern by BPTF via Multivalent Interactions. *Cell*. 2011; 145:692–706. [PubMed: 21596426]
- Ruthenburg AJ, Li H, Patel DJ, Allis CD. Multivalent engagement of chromatin modifications by linked binding modules. *Nat Rev Mol Cell Biol*. 2007; 8:983–994. [PubMed: 18037899]
- Schmitges, Frank W.; Prusty, Archana B.; Faty, M.; Stützer, A.; Lingaraju, Gondichatnahalli M.; Aiwazian, J.; Sack, R.; Hess, D.; Li, L.; Zhou, S., et al. Histone Methylation by PRC2 Is Inhibited by Active Chromatin Marks. *Molecular Cell*. 2011; 42:330–341. [PubMed: 21549310]
- Seenundun S, Rampalli S, Liu QC, Aziz A, Pali C, Hong S, Blais A, Brand M, Ge K, Dilworth FJ. UTX mediates demethylation of H3K27me3 at muscle-specific genes during myogenesis. *EMBO J*. 2010; 29:1401–1411. [PubMed: 20300060]
- Simon JA, Kingston RE. Mechanisms of polycomb gene silencing: knowns and unknowns. *Nat Rev Mol Cell Biol*. 2009; 10:697–708. [PubMed: 19738629]
- Simon MD, Chu F, Racki LR, de la Cruz CC, Burlingame AL, Panning B, Narlikar GJ, Shokat KM. The site-specific installation of methyl-lysine analogs into recombinant histones. *Cell*. 2007; 128:1003–1012. [PubMed: 17350582]
- Syka JEP, Marto JA, Bai DL, Horning S, Senko MW, Schwartz JC, Ueberheide B, Garcia B, Busby S, Muratore T, et al. Novel linear quadrupole ion trap/FT mass spectrometer: performance characterization and use in the comparative analysis of histone H3 post-translational modifications. *J Proteome Res*. 2004; 3:621–626. [PubMed: 15253445]
- Taverna SD, Li H, Ruthenburg AJ, Allis CD, Patel DJ. How chromatin-binding modules interpret histone modifications: lessons from professional pocket pickers. *Nat Struct Mol Biol*. 2007; 14:1025–1040. [PubMed: 17984965]
- Vermeulen M, Mulder KW, Denisov S, Pijnappel WWMP, van Schaik FMA, Varier RA, Baltissen MPA, Stunnenberg HG, Mann M, Timmers HTM. Selective anchoring of TFIID to nucleosomes by trimethylation of histone H3 lysine 4. *Cell*. 2007; 131:58–69. [PubMed: 17884155]
- Voigt P, Reinberg D. Histone Tails: Ideal Motifs for Probing Epigenetics through Chemical Biology Approaches. *ChemBioChem*. 2011; 12:236–252. [PubMed: 21243712]
- Wang Z, Zang C, Rosenfeld JA, Schones DE, Barski A, Cuddapah S, Cui K, Roh TY, Peng W, Zhang MQ, et al. Combinatorial patterns of histone acetylations and methylations in the human genome. *Nat Genet*. 2008; 40:897–903. [PubMed: 18552846]
- Xu M, Long C, Chen X, Huang C, Chen S, Zhu B. Partitioning of histone H3-H4 tetramers during DNA replication-dependent chromatin assembly. *Science*. 2010; 328:94–98. [PubMed: 20360108]
- Young MD, Willson TA, Wakefield MJ, Trounson E, Hilton DJ, Blewitt ME, Oshlack A, Majewski IJ. ChIP-seq analysis reveals distinct H3K27me3 profiles that correlate with transcriptional activity. *Nucleic Acids Research*. 2011; 39:7415–7427. [PubMed: 21652639]
- Young NL, DiMaggio PA, Plazas-Mayorca MD, Baliban RC, Floudas CA, Garcia BA. High throughput characterization of combinatorial histone codes. *Mol Cell Proteomics*. 2009; 8:2266–2284. [PubMed: 19654425]
- Yuan W, Xu M, Huang C, Liu N, Chen S, Zhu B. H3K36 Methylation Antagonizes PRC2-mediated H3K27 Methylation. *J Biol Chem*. 2011; 286:7983–7989. [PubMed: 21239496]

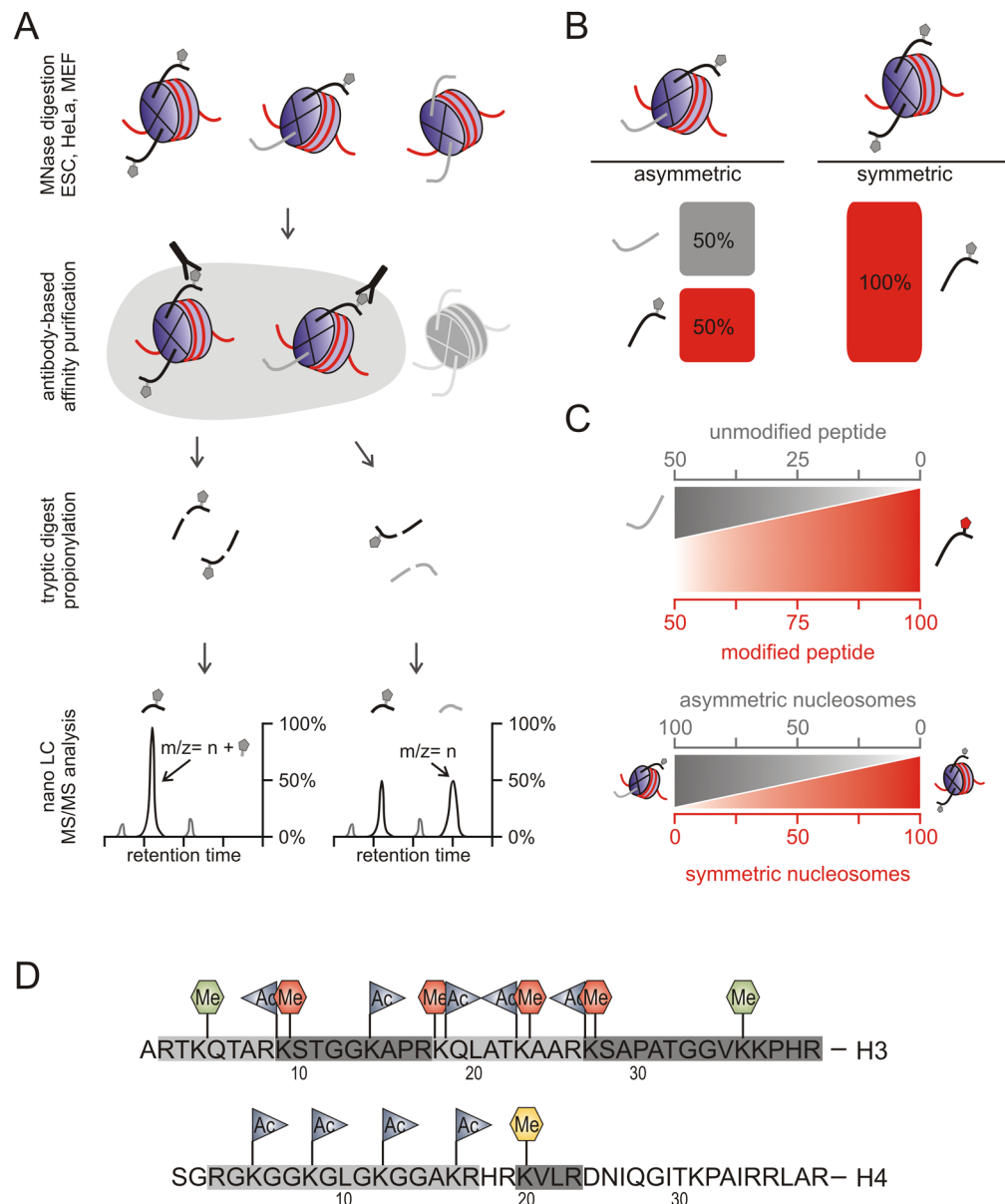


Figure 1. Analysis of Histone Modification Symmetry by Immunoaffinity Purification and Mass Spectrometry

A, Outline of the experimental approach. See main text for details. **B**, For a hypothetical binary (unmodified/modified) mark, asymmetric nucleosomes give rise to equal amounts of modified and unmodified peptide, whereas the symmetric case yields only the modified peptide. **C**, If a mixed population is present, the abundance of unmodified peptide decreases with increasing proportions of symmetric nucleosomes. The peptide quantification yields the relative amount of symmetric and asymmetric populations through interpolation between the limiting cases. **D**, Modifications covered in MS analysis. Tryptic peptides generated from propionylated histones H3 and H4 are shown along with detected acetylation and methylation sites. See also Figure S1.

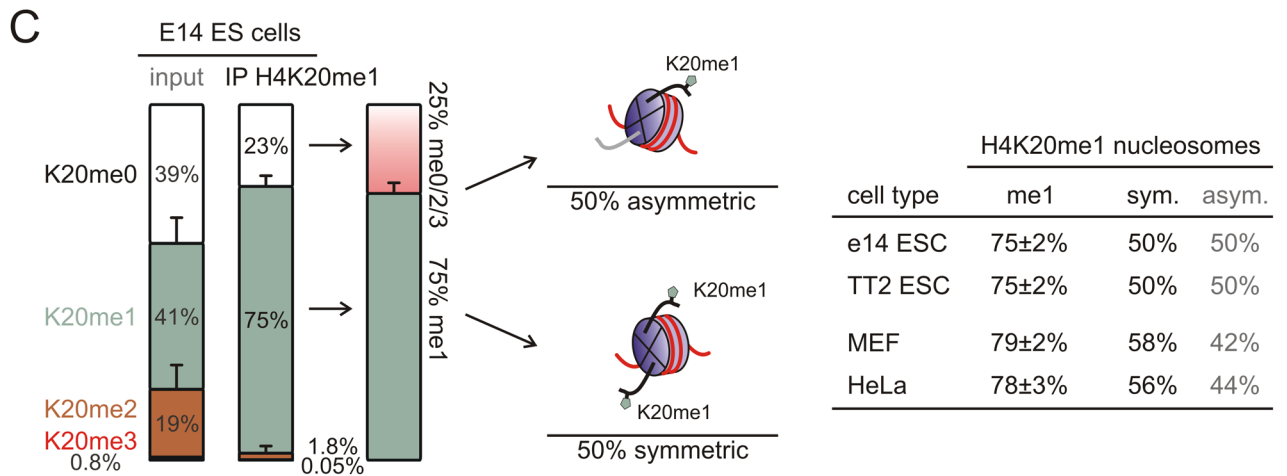
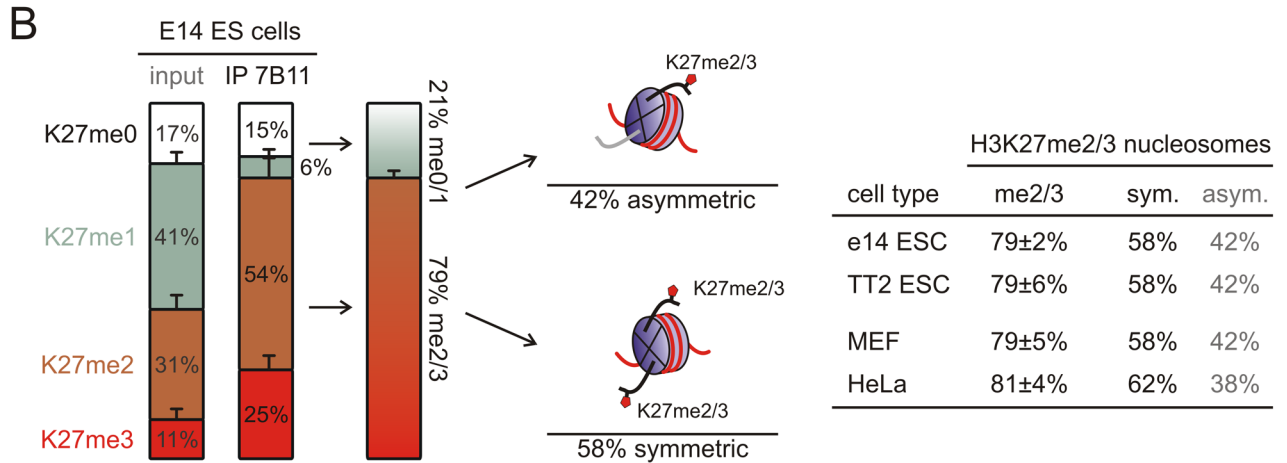
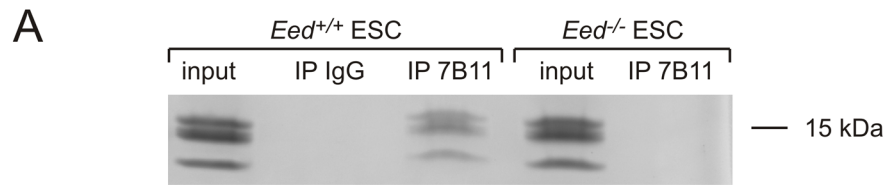


Figure 2. Nucleosomes are modified both symmetrically and asymmetrically with H3K27me2/3 and H4K20me1

A, Example of a mononucleosome affinity purification and specificity controls for an H3K27me2/3-specific antibody. **B**, **C**, Determination of symmetric and asymmetric populations for H3K27me2/3 (**B**) and H4K20me1 (**C**) based on quantitative LC-MS/MS data. Left panels show data for E14 ES cells, tables summarize data for the indicated cell types. Results represent average and SEM of at least two independent experiments based on two different nucleosome preparations per cell type. See also Figures S1, S2, and S3 and Table S2.

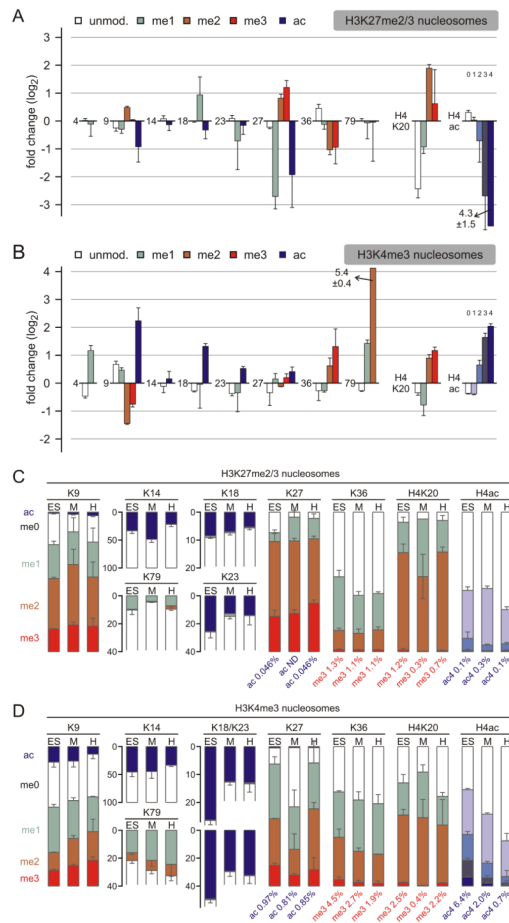


Figure 3. Co-occurrence of histone marks with H3K27me2/3 and H3K4me3 in ES, MEF, and HeLa cells

A, B, Modification profile of mononucleosomes prepared from E14 ES cells by H3K27me2/3 (**A**) or H3K4me3 (**B**) antibody-based affinity purification. Given are fold changes over input for the indicated sites and modification states on H3 and H4. For H4 acetylation, abundance of unacetylated – tetraacetylated species (H4ac0–4) as well as site-specific acetylation status (H4Kac5/8/12/16) is shown. Positive values denote co-enrichment, while negative values indicate an inverse correlation with the targeted site. Results represent average and SEM of at least two independent experiments each. **C, D,** Modification state of H3K27me2/3 and H3K4me3 mononucleosomes from ES cells, MEFs, and HeLa cells. Abundances of methylation and acetylation states are shown as stacked columns normalized to 100% for each site. Shown are averages of at least two independent experiments each. See also Figure S4 and Table S2.

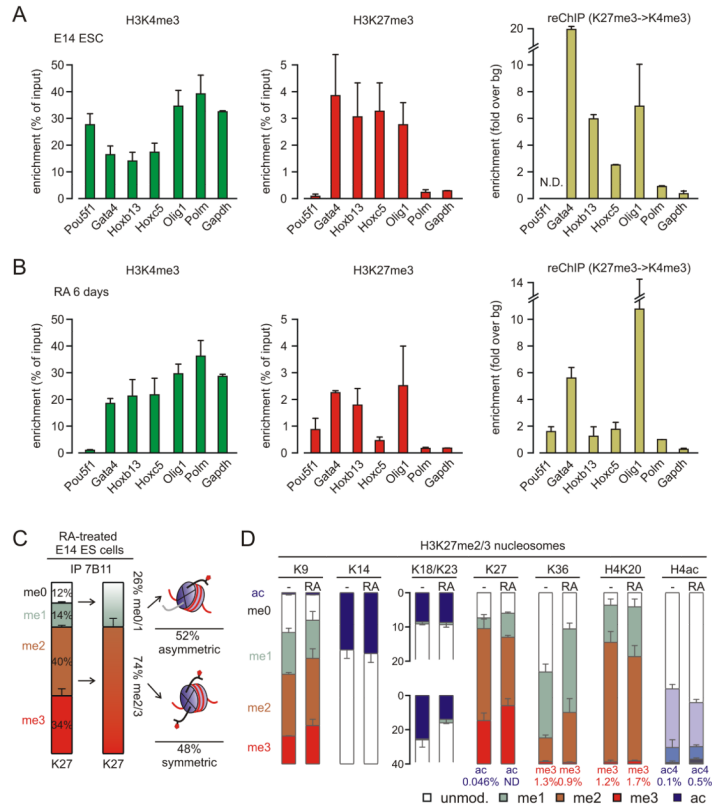


Figure 4. Sequential ChIP analysis of bivalent promoters in ES cells and modification state of H3K27me2/3 nucleosomes in differentiated ES cells

A, B, ChIP analysis of the indicated promoters with H3K4me3 and H3K27me3 antibodies. Right panel shows sequential ChIP with the H3K27me3 followed by H3K4me3 antibody. Assays were performed on untreated E14 cells (**A**) and E14 ES cells differentiated with retinoic acid (RA) for 6 days (**B**). The re-ChIP data is given as fold over IgG control in the second IP. Shown are means and SEM from two independent experiments. **C**, Mononucleosomes were affinity-purified from retinoic acid-treated cells with H3K27me2/3 antibody to assess their symmetry state as described in Figure 2. **D**, Modification profile of H3K27me2/3 nucleosomes immunopurified from retinoic acid (RA)-differentiated cells. For comparison, the modification state of E14 ES cells is given. Results represent mean and SEM of three independent experiments. See also Figure S2H, I.

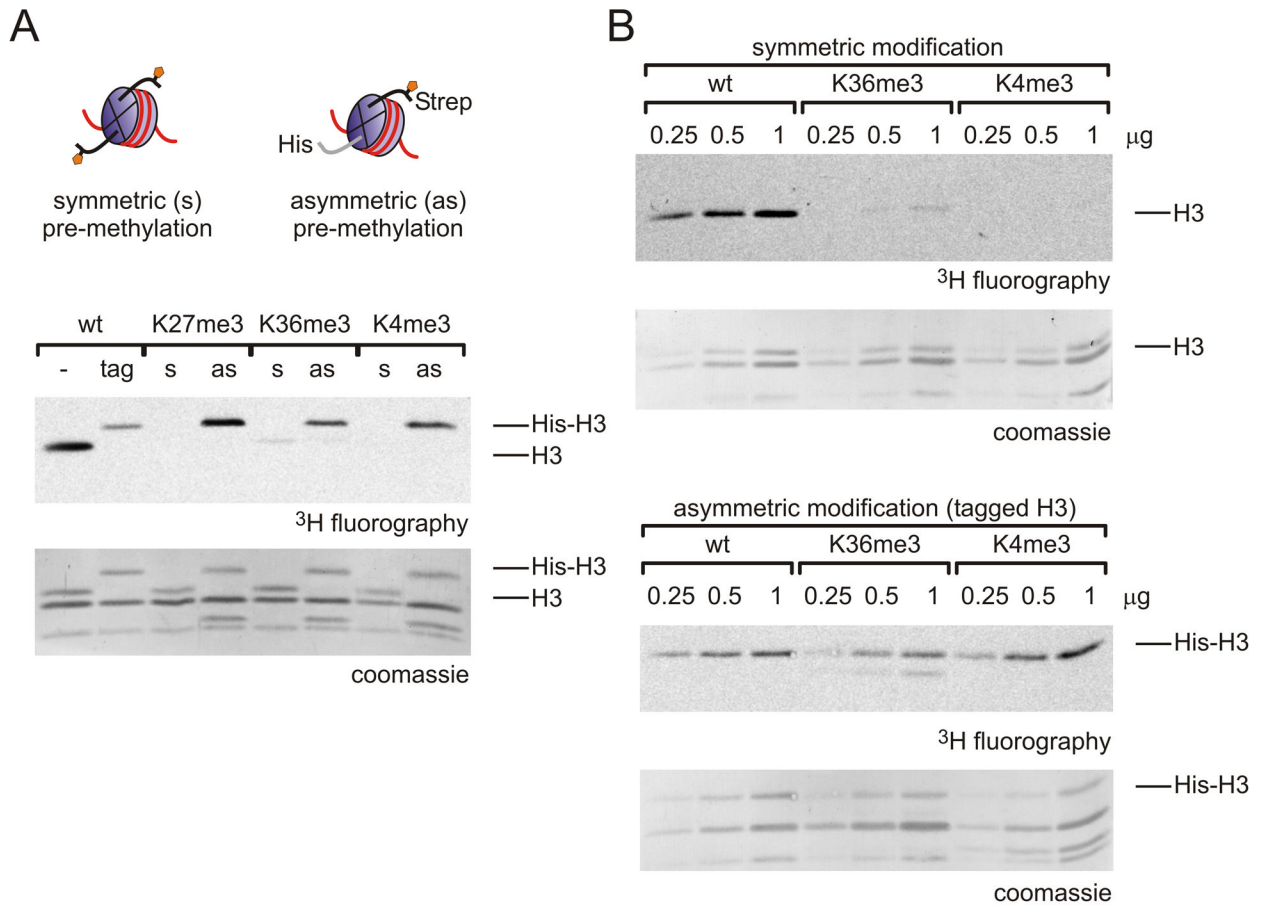


Figure 5. PRC2 is inhibited by symmetric, but not asymmetric, presence of H3K4me3 or H3K36me3

A, Histone methyltransferase assays on oligonucleosome substrates containing H3 with trimethyl-lysine analogues at the indicated positions either on both (s) or only one tail (as) per nucleosome. The asymmetric cases were generated using differentially tagged modified and unmodified histone H3 and double affinity purification. **B**, Titration of symmetrically and asymmetrically modified substrates. Panels shown are representative of three independent assays. See also Figure S5.

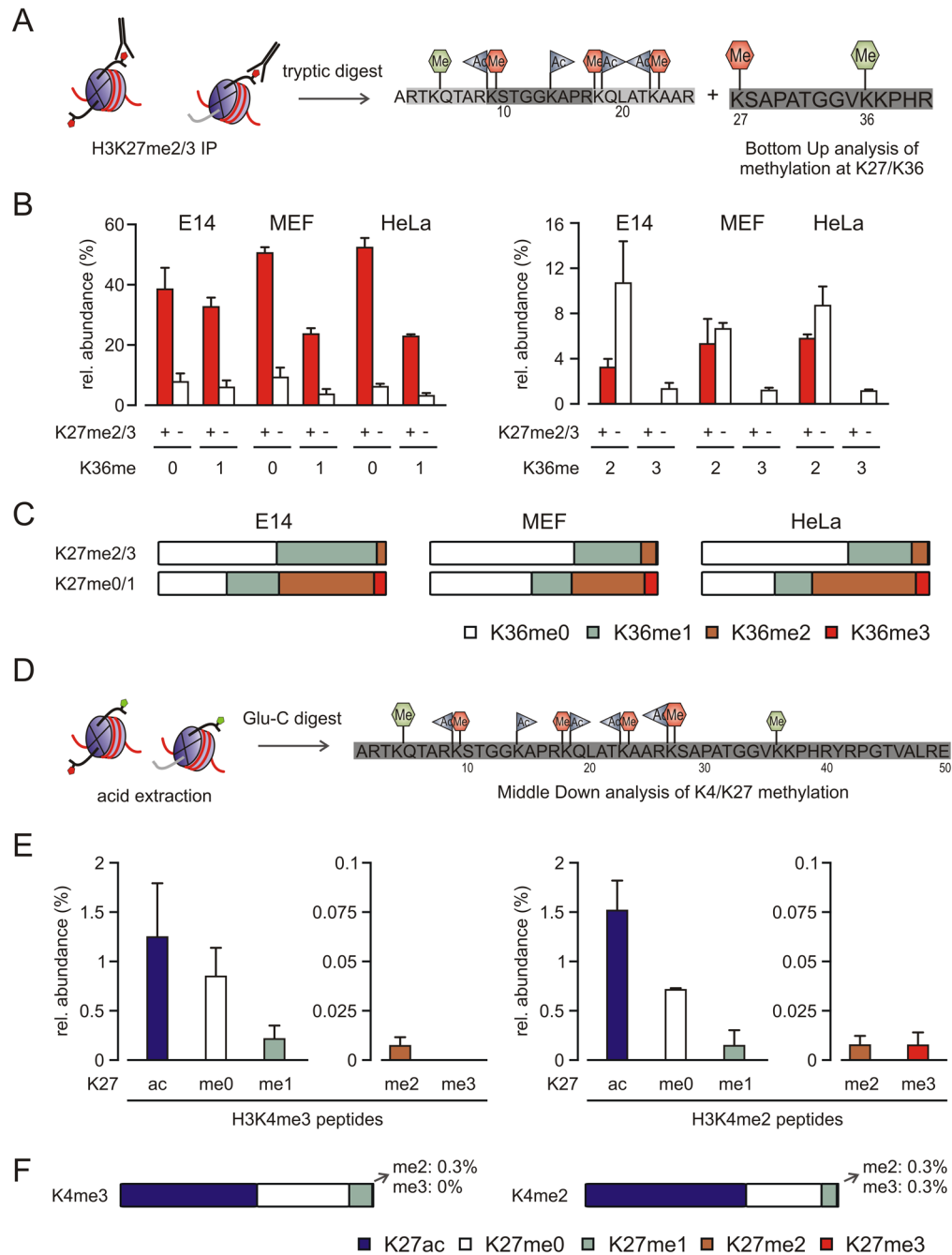


Figure 6. Bivalent Nucleosomes Contain H3K27me3 and H3K4me3/H3K36me3 on Opposing Tails *In Vivo*

A, Illustration of the experimental design. H3K27me2/3 nucleosomes are immunoaffinity-purified and subjected to Bottom Up LC-MS/MS analysis. H3K27 and H3K36 remain on the same peptide, allowing assessment of their interplay on single tails versus nucleosomes. **B**, The relative abundance of peptides detected is grouped according to modification status at H3K27 (open bars, unmodified or me1; red bars, me2, me3). Note the difference in y axis scale between the panels. Shown are means and SEM of at least three experiments each. **C**, Alternative representation of the data shown in B. To assess the relative abundance of H3K36 states in the presence or absence of H3K27me2/3, the percentage of H3K36 states

was normalized to the total abundance of peptides with or without H3K27me_{2/3}. **D**, Illustration of the Middle Down MS approach. Acid-extracted nuclear histones were subjected to Glu-C digest and the resulting H3.1(1–50) peptide was analyzed. **E**, Abundance of peptides containing H3K4me₃ and H3K4me₂ plotted as a function of H3K27 modification state on the same peptides. Peptides were assigned with custom-made software and manually validated in some cases. Shown are means and SEM of three experiments each. The error reflects both technical error of measurement and mis-assignment of peptide species by the software. **F**, Alternative representation of the data in E with peptide abundances normalized to the sum of all H3K4me₃/H3K4me₂ peptides.

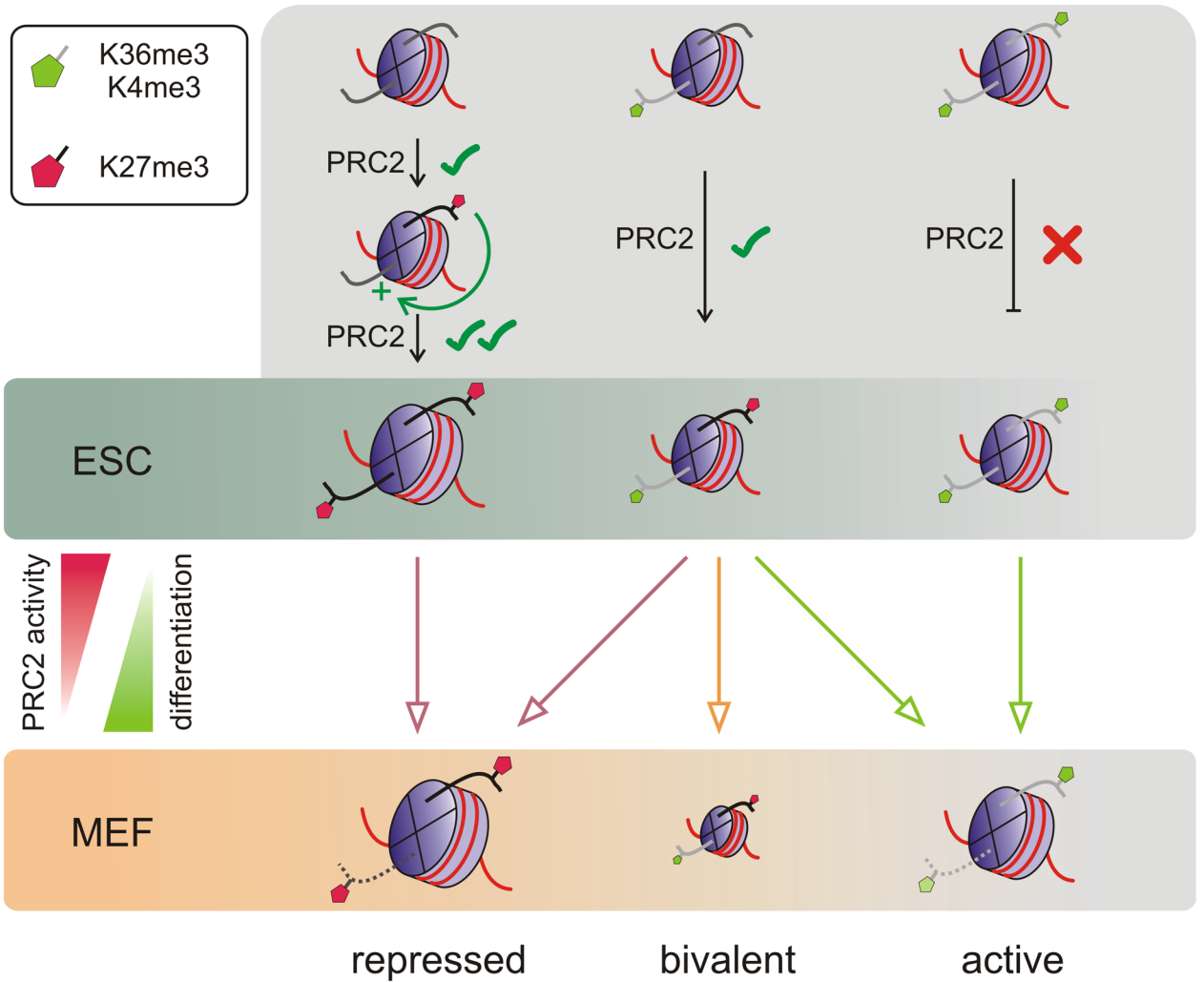


Figure 7. Model for the generation of symmetric and asymmetric nucleosomes by PRC2
 Schematic model showing modulation of PRC2 activity by active marks present on one or both copies of H3 per nucleosome as well as their possible fates in the transition from ES cells (ESC) to more differentiated lineages (such as MEFs). Scale of nucleosome symbols in the ESC and MEF panels reflects their relative abundance.